Relaxation between closely spaced electronic levels of rare-earth ions doped in nanocrystals embedded in glass

R. S. Meltzer, W. M. Yen, and Hairong Zheng
Department of Physics and Astronomy, The University of Georgia, Athens, Georgia 30602

S. P. Feofilov
A.F. Ioffe Physical-Technical Institute, 194021 St. Petersburg, Russia

M. J. Dejneka
Corning Inc., Corning, New York 14831

(Received 25 February 2002; revised manuscript received 17 June 2002; published 13 December 2002)

The relaxation between closely spaced (separation $\sim 10\ \mathrm{cm}^{-1}$) electronic levels of rare-earth ions doped in insulating nanocrystals (size 10–25 nm) embedded in glass is studied by time-resolved fluorescence and fluorescence line narrowing techniques. For particle sizes below 25 nm the relaxation rate increases with a decrease in particle size. The increased relaxation rate is explained by the interaction of the electronic states of rare-earth ions in nanocrystals with the vibrational excitations of the surrounding glass medium and with mixed vibrational modes of the nanocrystallites and the glass. The possibility for the use of rare-earth doped nanocrystals as a probe of the dynamical processes in glass is discussed.

DOI: 10.1103/PhysRevB.66.224202 PACS number(s): 78.67.Bf

I. INTRODUCTION

The dynamical properties of rare-earth (RE) ions doped into glasses (or disordered materials) are very different from the situation when the RE ions are doped into bulk single crystals. In the case of glasses, the dynamical properties are governed by the interactions with the two-level systems (TLS's) and the localized vibrational excitations of the glass matrix (see Refs. 1–4 for reviews). It is also known for ''free-standing'' nanoparticles consisting of loosely packed nanocrystalline clusters, that the electron-phonon interaction of RE ions contained in the nanoparticles is strongly modified compared to that of the bulk. For example, the electronic relaxation rate among closely spaced energy levels in small nanoparticles resulting from the single-phonon direct process can experience a significant reduction due to the gap in the acoustic-phonon spectrum and the reduction in the phonon density of states.[5,6] In addition, it has been demonstrated for nanoparticles that optical dephasing resulting from two-phonon Raman processes can be enhanced and its temperature dependence modified by confinement of the phonon modes and the alteration in the phonon density of states resulting from confinement.[7,8]

In the present paper, we address the question of what processes dominate the electronic relaxation between the closely spaced (separation $\sim 10\ \mathrm{cm}^{-1}$ or ~ 100 GHz) electronic levels of RE ions contained in nanoparticles when these particles are embedded in a glass matrix. It has proven very difficult to probe the direct process for RE ions in glasses using optical techniques because the inhomogeneous broadening makes it very difficult to study populations of specific crystal-field levels. This inhomogeneous broadening leads to a wide energy distribution of crystal-field levels and as a result to broad spectra in which the individual crystal field levels are not resolved. However, for RE ions doped into insulating nanoparticles, sharp line optical spectra remain and these spectra are essentially identical to those of the structurally identical bulk single crystals. This occurs because the RE spectra are governed by the local environment which is the same for all RE ions in the nanocrystals as is the case for bulk crystals. However, for electronic relaxation of RE ions doped in nanoparticles surrounded by the glass, long-range interactions may make it possible for the single-phonon direct process involving the phonon modes of the glass to make an important contribution to the relaxation rate. Indeed, their exist two examples for which the long-range interactions of the RE ions and the glass are known: (i) the modified radiative lifetime of the excited states of RE ions in nanoparticles due to local-field effects and the altered effective index of refraction of the media,[9,10] and (ii) the ''glasslike'' homogeneous broadening of the electronic transitions of RE ions in nanoparticles, which is due to elastic dipole-dipole interactions between RE ions in the nanoparticles and the TLS in the glass.[11,12]

When considering the population relaxation among electronic levels of RE ions doped in nanoparticles that are embedded in glass, two modifications relative to the single-phonon direct process in bulk crystals need to be considered: (i) the modification of the vibrational spectrum of the nanoparticles due to size restriction, and (ii) the role of the interaction with the vibrational excitations of the glassy matrix. The goal of our experiments was to determine the dominant mechanism of relaxation. The results of such a study may also provide information on the direct relaxation in RE centers directly embedded in glass that would extend the very limited frequency range (~ 10 GHz) known from electron paramagnetic resonance (EPR) experiments on spin-lattice relaxation in glass[13,14] to much higher frequencies. This work is also motivated by the interest in determining the optical properties of these interesting materials, RE doped oxyfluoride glass ceramics, which may have important applications.[15]

The dynamics are studied both in the time and frequency domain as a function of particle size. Pulsed laser excitation of specific electronic levels of Ho^{3+} ions embedded in the nanoparticles is used to prepare nonequilibrium populations of specific states and these populations are monitored with time-resolved fluorescence. Enhanced relation rates are observed for nanoparticles smaller than 25 nm. In addition, fluorescence line narrowing (FLN) experiments are performed on Pr^{3+} to measure the homogeneous linewidths from which the relaxation rates are obtained. While the FLN measurements are identical to those of the bulk for the smallest nanoparticles we were able to study (23 nm), this result sets an upper limit on the particle size for which electronic relaxation rates are significantly affected by interactions with the surrounding glass matrix.

II. EXPERIMENT

The experiments were performed with transparent oxyfluoride glass ceramics[15] consisting of the glassy matrix, in which 10–25 nm Ho^{3+}- or Pr^{3+}-doped LaF_3 crystallites are embedded. The size of the nanocrystals in the glass ceramics could be controlled by annealing the samples at different temperatures. The samples were held at 650 °C for 4 h to nucleate the crystals and then held at the final temperature (700, 750, 775, 800, or 825 °C) for 4 h to grow the crystals to the desired size. Electron and atomic force microscopy and x-ray diffraction were used for measurements of the size of the nanocrystals. A measurement of the average crystallite size is repeatable to ± 1.0 nm and 90% of the particles are within 7.5 nm of the average. The average RE concentration in the oxyfluoride ceramic samples was 0.1% for Ho-doped and 0.05% for Pr-doped samples, but the RE concentration in the nanocrystals is usually a few times higher due to RE segregation. However, some of the RE ions are always present in the glass component.

The samples were mounted in a liquid-helium cryostat. In the spectroscopic and the time-resolved fluorescence measurements the samples were excited with a pulsed dye laser pumped with the second harmonic of a *Q*-switched YAG:Nd laser (Quanta Ray, pulse duration 10 ns, repetition rate 10 Hz). The laser light was loosely focused (~0.5–1 mm) on the samples. For the high temporal resolution measurements the laser light was filtered with a monochromator in order to decrease the broadband dye fluorescence/superradiance reaching the samples. The fluorescence was analyzed with a single- or double-grating monochromator and detected with a photomultiplier tube. For the time-resolved measurements the data were stored and averaged in a multichannel scaler (EG&G, 5 ns temporal resolution) or a digital oscilloscope (lower temporal resolution).

For the fluorescence line narrowing experiments a cw dye laser, Coherent CR599 (frequency jitter ~2 MHz), provided ~30 mW resonant with the Pr^{3+} $^3H_4-{}^1D_2$ transition. The resonant FLN fluorescence was selected with an interference filter and analyzed with a scanning Burleigh RC-140 Fabry-Perot interferometer. The signal was detected with a photomultiplier and was stored in a digital oscilloscope. In order to block the laser excitation light from the detection system, the exciting laser light was chopped by an acousto-optic modulator (AOM) which was electronically synchronized with the chopper wheel in the fluorescence collection path. The electronic delay was aligned so that the input pinhole at the auxiliary waist of the fluorescence collection beam was blocked when the AOM opened the laser light path to the sample and vice versa. The light on/off periods were <0.5 ms, which, because of the ~0.6-ms $^1D_2$ state lifetime of Pr^{3+}, allowed observation of the resonant FLN signal. The Fabry-Perot interferometer free spectral range was set at 5, 10, 20, or 50 GHz, as appropriate for the measurement. Between each FLN measurement the AOM-chopper delay was changed and scans were taken of the scattered laser light in order to determine the interferometer resolution. The FLN data were corrected for the instrumental contribution to the measured linewidths.

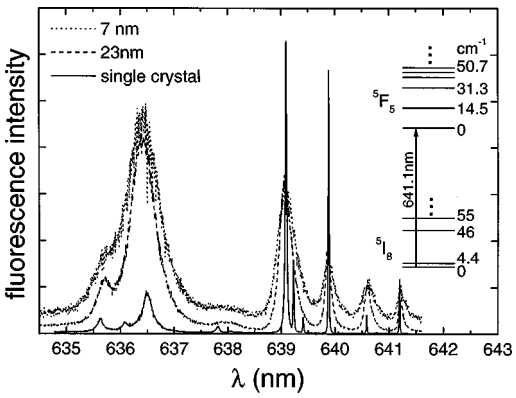

FIG. 1. The excitation spectra of Ho^{3+} $^5F_5-{}^5I_8$ fluorescence ($\lambda = 643.2$ nm) in oxyfluoride glass ceramics containing $LaF_3:Ho^{3+}$ nanocrystals of different size and of $LaF_3:Ho^{3+}$ single crystal (intensities adjusted for clarity of presentation). Inset: energy level scheme (simplified) of $^5F_5$ and $^5I_8$ states of Ho^{3+} in LaF_3.

III. EXPERIMENTAL RESULTS AND DISCUSSION

A. Optical spectra and thermal relaxation of nonequilibrium vibrational excitations in oxyfluoride glass ceramics

The excitation and fluorescence spectra of the Ho^{3+} $^5F_5-{}^5I_8$ transition in oxyfluoride glass ceramics containing $LaF_3:Ho^{3+}$ nanocrystals are shown in Figs. 1 and 2, respectively. Also shown are the crystal-field sublevels of the two manifolds. The samples were immersed in liquid helium at $T = 1.5$ K. It can be seen in Fig. 1 that the excitation spectra of $LaF_3:Ho^{3+}$ nanocrystals are similar to that of the bulk single crystal, which is shown for comparison. The main differences are the significantly larger inhomogeneous broadening of the spectral lines in the glass ceramic samples and the existence of a broad fluorescence background resulting from the presence of some RE ions contained directly in the glassy component of the samples. The increase in the inhomogeneous broadening with a decrease of nanoparticle size may be due to the increasing fraction of the RE ions close to the crystallite surface as the particle size is reduced or to the higher concentration of defects in the smaller nanoparticles.

Before considering the rapid relaxation of the nonequilibrium population of electronic states produced by the resonant

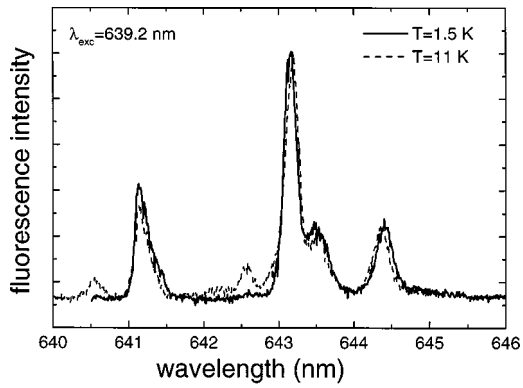

FIG. 2. The fluorescence spectra of Ho^{3+} $^5F_5-^5I_8$ transition in oxyfluoride glass ceramics containing $LaF_3:Ho^{3+}$ nanocrystals ($\lambda_{exc}=639.2$ nm).

laser excitation, one should consider the thermal conditions of the nanocrystals and surrounding glass produced by the absorption of light energy. This is necessary in order to understand the quasiequilibrium state of the ceramic that exists after this rapid relaxation. The absorption of light occurs both in the nanocrystals and in the glass through resonant absorption of the electronic states of the rare-earth ions. Assuming the same concentration of rare-earth ions in the nanocrystals and glass, we estimate that at least 90% of the resonantly absorbed energy resides in the nanoparticles despite the fact that they occupy only about 10% of the volume. This follows from the 100-fold larger inhomogeneous width of the rare-earth ion resonances in the glass relative to that in the nanocrystals which implies that only 0.01 as large a fraction of the ions are resonant with the laser in the glass as compared to the nanocrystal. Actually, since the concentration of RE ions is significantly higher in nanocrystals than in glass,[15] the fraction of energy absorbed in the nanocrystals may be even greater. A significant fraction of the electronic energy created in the absorption is converted into thermal energy (phonons) due to nonradiative processes which occur either directly from the initially excited states or from excited terminal levels that result from the radiation to these lower excited levels. Assuming similar quantum efficiencies in the nanocrystals and glass, it follows that the thermal energy density in the nanocrystals is much larger. The resulting phonons will be rapidly transported to the glass. The time scale for the achievement of a quasiequilibrium between the vibrational excitations in the nanoparticles and those in the surrounding glass is difficult to estimate. The equilibration process is complicated by a number of factors such as the microscopic elastic properties of the nanocrystal/glass interface, the acoustic mismatch between the crystalline and glassy materials, and the larger density of the vibrational states in the glass (localized vibrations) compared to that in the nanoparticles. To our knowledge the rate of the phonon transfer between the nanoparticles and the surrounding glass has never been measured experimentally, though some related parameters were determined in Ref. 16 for silicon nanocrystals embedded in amorphous Si. However, we estimate that this is rapid relative to the thermal relaxation of the excited volume of the ceramic.

The resulting frequency distribution of optically generated vibrational excitations (''phonons'') in the excited volume of the glass samples containing the nanoparticles after the intense laser excitation could differ significantly from that corresponding to the 1.5-K temperature of the liquid-helium bath.[17,18] The distribution of the vibrational excitations in the optically excited glass is usually nonequilibrium and cannot be characterized with a single temperature.[17,18] It is customary to define a frequency-dependent effective temperature derived from the occupation numbers of the vibrational excitations at a given frequency. Thus the dynamics of the vibrational excitations distribution in glass is better characterized by the occupation numbers of phonons at each frequency. The phonon distribution in the excited volume of the sample decays to the 1.5-K values by the diffusion of phonons out of the excited volume accompanied by anharmonic decay of the phonons.

The fast equilibration of vibrational excitations in nanoparticles and in glass offers the opportunity to use the nanoparticles to monitor the phonon excitation of the glass. We studied the vibrational excitation dynamics in the excited volume at the phonon frequency resonant with the lower level of the $^5F_5$ excited state (14.5 cm^{-1}) using the technique of optical detection of phonons.[19] In this method, the relative populations of two electronic states coupled by the phonons is determined. The phonon occupation numbers are derived from these populations and the effective temperature may be then defined from the Boltzmann factor describing these relative populations. The laser was tuned so as to selectively induce transitions from the ground state to the different excited sublevels of the $^5F_5$ state of Ho^{3+} in LaF_3 nanocrystals (inset of Fig. 1), e.g., the 14.5-cm^{-1} level with $\lambda_{exc}=640.5$ nm and the 31.3-cm^{-1} level with $\lambda_{exc}=639.2$ nm. The fluorescence from the second sublevel of the excited $^5F_5$ state of Ho^{3+} ions (at $\lambda=640.5$ or 642.6 nm, see inset in Fig. 1) in nanocrystals was used as a probe of the occupation numbers of 14.5-cm^{-1} vibrational excitations in the excited volume. The long (550 μs) radiative lifetime of the $^5F_5$ excited state makes it possible to detect the fluorescence for more than 2 ms after the laser pulse. The decay of the fluorescence from transitions originating from the lowest sublevel (intensity I_1) and the first excited sublevel at 14.5 cm^{-1} (intensity I_2) of the $^5F_5$ excited manifold was observed after the pulsed laser excitation. The time-dependent occupation number of 14.5-cm^{-1} vibrational excitations in the excited volume was obtained from the ratio of the intensities $I_2(t)/I_1(t)$. Since the observed decay of fluorescence from both sublevels can be well described as exponential, the decay time of the 14.5-cm^{-1} vibrational excitations is well defined. In Fig. 3 this decay time (squares) is plotted vs the laser pulse energy for two different excitation frequencies. The measured decay time and its dependence on the laser pulse energy is in good agreement with other optical studies of nonequilibrium vibrational excitations generated by laser pulses in glass.[18] This result shows that the RE doped nanoparticles may serve as fluorescent probes of the relatively slow vibrational excitation dynamics in the glass.

The effective temperature of the excited volume is defined from the Boltzmann population ratio among the first two

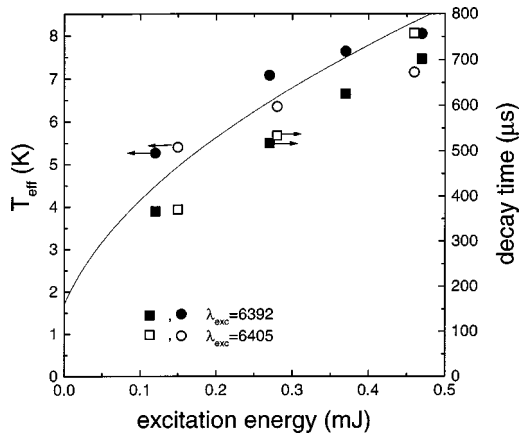

FIG. 3. The dependence of the vibrational excitations decay time and of the effective temperature on the laser pulse energy for two different excitation frequencies.

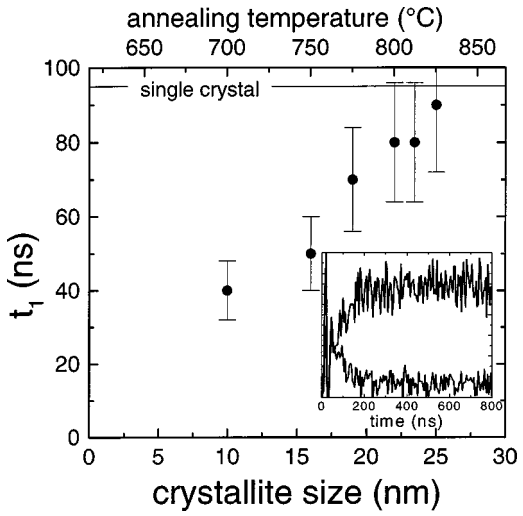

FIG. 4. Times of relaxation between the two lowest $^5F_5$ state sublevels of Ho^{3+} in nanocrystals of different sizes embedded in oxyfluoride glass ceramics. Solid line: the relaxation time value for single crystal. Inset: typical time-resolved fluorescence decay and buildup curves.

sublevels of the $^5F_5$ manifold separated by $\Delta E = 14.5\ \mathrm{cm}^{-1}$, $N_2/N_1 = \exp(-\Delta E/kT_{\mathrm{eff}})$, which is obtained from the ratio of the fluorescence intensities. To convert from intensity ratio to population ratio, the fluorescence spectra were obtained at a known elevated temperature with very low laser excitation power ($<10\ \mu$J) such that no optical heating is observed (see Fig. 2) so as to determine the relative transition probabilities for the two transitions. In this spectrum the fluorescence from the higher excited state sublevels due to their thermal population is observed at $\lambda = 640.5$ and 642.6 nm. In Fig. 3 (circles) the effective temperature measured for 14.5-cm^{-1} vibrational excitations, shortly after the excitation pulse, is plotted vs the laser pulse energy for two different excitation frequencies. The observed effective local temperature of the nanoparticles at 14.5 cm^{-1} falls in the range of 4–8 K. It is expected that the phonons are in quasithermal equilibrium with the surrounding glass and it is found that the excited volume cools only on a millisecond time scale. The solid line in Fig. 3 represents the theoretical prediction that the temperature of the nanoparticles varies as the square root of the laser power, a behavior that is expected if the nanoparticle and the local volume of the glass matrix surrounding the nanoparticle (assumed to be much larger than the volume of the nanoparticle) are at the same effective temperature and that the heat capacity of glass at low temperatures varies linearly with temperature. It should be noted that the effective temperature, determined from a measurement of the phonon occupation numbers at different frequencies, may be frequency dependent because the real frequency distribution of vibrations in the optically excited glass may be nonequilibrium.

B. Relaxation between the $^5F_5$ excited state sublevels of Ho^{3+} in LaF_3 nanocrystals in glass

The direct observation of the relaxation between the two lowest $^5F_5$ sublevels was performed under excitation of the upper sublevel at $\lambda = 640.5$ nm. Transitions from both sublevels to one of the ground $^5I_8$ state components were observed in fluorescence at $\lambda = 642.6$ nm and $\lambda = 643.2$ nm which served as a measure of the sublevel populations. Initially after excitation, the population of the Ho^{3+} ions is predominantly in the second sublevel, 14.5 cm^{-1} above the metastable state (see Fig. 1). The population then decays through the single-phonon direct process producing a 14.5-cm^{-1} phonon and an ion in the lower level. The time dependence of the luminescence decay of the upper level and the buildup of the emission from the lower level (5-ns temporal resolution) reveal the single-phonon decay rate (see inset in Fig. 4). The populations will relax to a quasiequilibrium value given by the effective temperature, as discussed above. Because the 14.5-cm^{-1} splitting between the excited state sublevels (phonon energy) is large compared to the excited volume effective temperature T_{eff}, which in these experiments was estimated as 5 K, it is easily possible to follow the direct process relaxation of the phonon occupation. The relaxation times were determined from both the higher sublevel decay and lower sublevel buildup curves and the average values were used to find the experimental relaxation times t_1. These relaxation times as a function of the size of the nanoparticles embedded in the oxyfluoride glass ceramics are shown in Fig. 4. The corresponding annealing temperatures are shown on the top axis. The value of t_1 decreases with a decrease of the nanocrystal size, whereas for the largest nanoparticles it approaches the single-crystal value.

The observed dependence of the relaxation time on nanocrystals size may be explained assuming an important role for the interaction of the electronic states of RE ions in the nanoparticles with the excitations of the glass matrix. In glass, low-lying vibrational modes of a nonacoustical nature are present.[3,20] These are responsible for an enhancement of the density of vibrational states relative to that in crystals. It is well known that the interaction with these modes makes a contribution to the homogeneous broadening of optical transitions for impurity ions in glass.[1,3] The excitation of these modes may also be the dominant mechanism in the direct

relaxation process between the closely spaced levels of RE ions in the nanocrystals embedded in glass.[14] At the frequency of 14.5 cm^{-1} (0.44 THz) the density of vibrational states of the glass is significantly greater than the density of states in crystals, at this same frequency, based on a Debye model.[3,20] The vibrational modes of the glass may, together with the phonon modes of nanoparticles, form new mixed vibrational states, which may take part in the single-phonon direct relaxation process. The exact nature of these states and their vibrational wave functions are not known and their interaction with the RE ions will depend on the location of these ions with respect to the surface of the nanoparticle. An additional relaxation mechanism connected with the interaction of RE ions with TLS's cannot be excluded though they are usually considered dominant in processes having smaller characteristic energies. In any case, the experimental results of Fig. 4 clearly suggest that the interaction with the glassy matrix becomes significant for the nanocrystals smaller than 25 nm and that these new modes lead to enhanced single-phonon relaxation rates.

C. Fluorescence line narrowing measurements of relaxation between the $^1D_2$ excited state sublevels of Pr^{3+} in LaF_3 nanocrystals in glass

Whereas in the previously discussed experiments the relaxation processes were examined in the time domain, the technique of fluorescence line narrowing (FLN) enables one to measure the relaxation rate in the frequency domain by obtaining the homogeneous linewidth of optical transitions. In FLN experiments, one excites a subset of ions within the inhomogeneously broadened absorption line and observes the resonant fluorescence of those ions. The observed linewidth is determined both by population relaxation and pure dephasing. Here, experiments were performed with oxyfluoride glass ceramics containing Pr^{3+} doped LaF_3 nanocrystals. In this host, the two lowest $^1D_2$ excited state crystal-field Stark components of Pr^{3+} in LaF_3 are separated by 23 cm^{-1}. The transition from the upper sublevel to the ground state (π polarized) lies at 591.7 nm, whereas the transition from the lower sublevel (σ polarized) is at 592.5 nm, see inset in Fig. 5. FLN studies[21] in bulk $LaF_3:Pr^{3+}$ single crystals showed that the width of the π (upper) transition, below 10 K, is determined by one-phonon relaxation to the lower excited state sublevel with the emission of a 23-cm^{-1} phonon. When the nanocrystals are embedded in the glass, there may be an additional contribution to the relaxation associated with interaction of the Pr^{3+} ion with the surrounding glass medium. A comparison of the homogeneous broadening of $^1D_2-^3H_4$ π transition $\gamma_h=\gamma_{FLN}/2$ of Pr^{3+} in LaF_3 single crystals and in nanocrystals embedded in glass makes it possible to determine the contribution of the interaction with the vibrational modes of the glass to the relaxation process.

The temperature dependence of the homogeneous linewidth of the $^1D_2-^3H_4$ π transition in $LaF_3:Pr^{3+}$ 23-nm nanocrystals in oxyfluoride glass ceramics doped with 0.05% Pr is shown in Fig. 5. For comparison, the data taken with a LaF_3:0.1% Pr^{3+} single crystal are also plotted. The thin

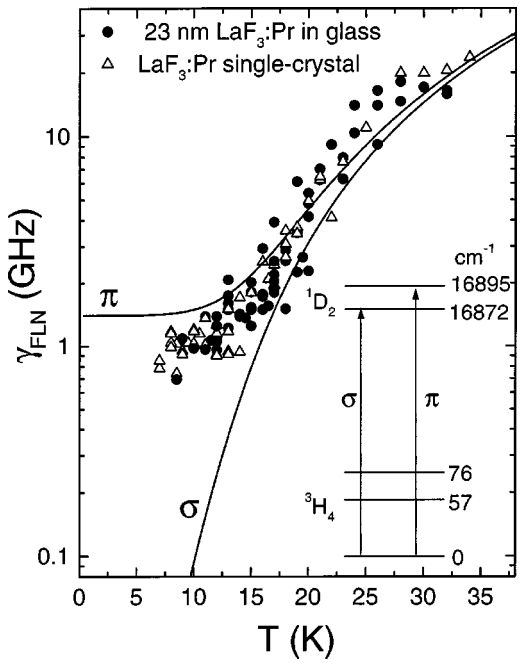

FIG. 5. Temperature dependence of the fluorescence line narrowed width for Pr^{3+} in LaF_3 nanocrystals embedded in oxyfluoride glass ceramics and for Pr^{3+} in LaF_3 single crystals. Thin solid lines: theoretical curves from Ref. 21.

solid lines are the theoretical curves[21] taking into account the one-phonon processes between the electronic states' sublevels. The temperature range of the experiment on the π transition was limited from the low-temperature side by the decrease of Boltzmann population of the upper excited state sublevel whose fluorescence became too weak to measure below about 6 K. The inherent weakness of the σ transition prevented us from making FLN measurements on it. These experiments were made more difficult by the fact that the FLN signals in Pr-doped glass ceramics are much weaker than in single crystals, due mostly to the larger inhomogeneous broadening of the transitions. (This also makes it impossible to perform experiments with smaller nanoparticles since the fluorescence becomes even weaker.) No observable difference between the homogeneous linewidth of the π transition for the embedded nanocrystals and in single crystals was observed. Nevertheless, this places an upper limit of 5×10^8 s^{-1} on the contribution to the relaxation rate of interaction with the vibrational states of glass at 23 cm^{-1} for 23-nm particles. This FLN result is consistent with the results on Ho^{3+} in the time-domain where it was found that 25 nm was the lowest size of nanoparticle where interactions with the modes of the glass could be observed (10% increase in the relaxation rate compared to the bulk). Although the direct process relaxation rate is not significantly increased for 25-nm particles, the elastic dipole-dipole interaction with the two-level systems of glass does significantly modify the pure dephasing rate as seen in previously reported measurements of the homogeneous linewidth of the σ transition using spectral hole burning, even at $T<5$ K in the same samples.[12] However, the hole burning experiments allow one to perform

much higher resolution linewidth measurements than FLN to make the interaction observable.

IV. CONCLUSIONS

It has been demonstrated that RE doped nanoparticles may serve as efficient probes of many dynamical processes in glass that cannot be observed when the RE ions are embedded directly in the disordered glass matrix.

The direct relaxation processes between the closely spaced electronic levels of RE ions in nanoparticles embedded in glass were studied. It is suggested that if the nanoparticles are small enough, the relaxation between the levels occurs with the generation of a vibrational excitation of glass or of the mixed nanoparticle-glass modes. The modification of the vibrational spectrum of nanoparticles due to size restriction effects, which results in the slowing down of the one-phonon direct relaxation in ''free-standing'' nanoparticles[5,6] does not play a significant role for the nanoparticles in glass. This may be explained by the damping and propagation into the glass of the size-resonant vibrations of the nanoparticles in the situation when the acoustic mismatch between the crystallite and the glass is small. Also, the size of the nanoparticles may be too large to produce significant modification of the vibrational density of states at the frequencies studied here.

The faster relaxation between the RE sublevels in smaller nanocrystals implies, that for ions present directly in the glass, an even faster relaxation must occur. Extrapolation of the results of Fig. 4 suggests that the relaxation rate of levels separated by 14.5 cm^{-1} may be at least three times but perhaps as much as an order of magnitude faster for ions in the glass than for those in the bulk crystals. This result is in agreement with the expected larger density of low-frequency vibrational states in glass compared to that in crystals.

For ions located directly in glass, the measurement of the direct relaxation processes between the closely spaced (separation ~ 10 cm^{-1}) electronic levels is difficult in optical experiments because of experimental difficulties connected with the large inhomogeneous distribution of energy level spacings in glass. However, utilizing the narrow distribution of energy-level separations and the sharpness of the optical transitions of the rare-earth ions in the nanocrystals, it was possible to circumvent these experimental problems and to use the nanocrystal size to vary the distance between the probe ions and the modes of the glass to which the RE ions couple. The results of the current study are in agreement with the increased spin-lattice relaxation rates for ions in glass compared to crystals observed in EPR (Refs. 13 and 14) for lower frequencies. Clearly, theoretical models for the vibrational modes of the nanoparticles imbedded in glass are needed to quantitatively understand the observed size dependence.

Using time-resolved fluorescence spectroscopy of RE ions in nanoparticles it was also possible to observe the dynamics of a distribution of nonequilibrium vibrational excitations (''phonons'') in glass and to determine the effective temperature of the optically excited sample volume. The small size of the nanoparticles ensures a fast enough response of the occupation of the energy levels of the RE ions to the changes in the effective temperature of the glass on the slower time scale of the glass thermalization. Thus the RE doped nanoparticles may be used as ''nanoscale thermometers'' in different media.

ACKNOWLEDGMENTS

We thank I. N. Kurkin for helpful discussion and the National Science Foundation, Grant DMR-9871864 for support of this research.

[1] J. Lumin. **36**, N4&5, special issue (1987).
[2] J. Friedrich and D. Haarer, in *Optical Spectroscopy of Glasses* edited by I. Zschokke (D. Reidel, Dordrecht, 1986), p. 149.
[3] D. L. Huber, Mater. Sci. Forum **50**, 77 (1989).
[4] J. L. Skinner and W. E. Moerner, J. Phys. Chem. **100**, 13 251 (1996).
[5] H.-S. Yang, S. P. Feofilov, D. K. Williams, J. C. Milora, B. M. Tissue, R. S. Meltzer, and W. M. Dennis, Physica B **263**, 476 (1999).
[6] H.-S. Yang, K. S. Hong, S. P. Feofilov, B. M. Tissue, R. S. Meltzer, and W. M. Dennis, J. Lumin. **83–84**, 139 (1999).
[7] S. P. Feofilov, A. A. Kaplyanskii, R. I. Zakcharchenya, Y. Sun, K. W. Jang, and R. S. Meltzer, Phys. Rev. B **54**, 3690 (1996).
[8] K. S. Hong, R. S. Meltzer, S. P. Feofilov, R. I. Zakharchenya, W. Jia, H. Liu, B. Tissue, and H. B. Yuan, J. Lumin. **83–84**, 393 (1999).
[9] R. S. Meltzer, S. P. Feofilov, B. Tissue, and H. B. Yuan, Phys. Rev. B **60**, R14 012 (1999).
[10] R. S. Meltzer, W. M. Yen, Hairong Zheng, S. P. Feofilov, M. J. Dejneka, B. Tissue, and H. B. Yuan, J. Lumin. **94–95**, 217 (2001).
[11] R. M. Macfarlane and M. J. Dejneka, Opt. Lett. **26**, 429 (2001).
[12] R. S. Meltzer, W. M. Yen, Hairong Zheng, S. P. Feofilov, M. J. Dejneka, B. Tissue, and H. B. Yuan, Phys. Rev. B **64**, 100201(R) (2001).
[13] A. Deville, A. Gaillard, and C. Blanchard, J. Phys. (France) **44**, 77 (1983).
[14] S. B. Stevens and H. J. Stapleton, Phys. Rev. B **42**, 9794 (1990).
[15] M. J. Dejneka, MRS Bull. **23**, 57 (1998); J. Non-Cryst. Solids **239**, 149 (1998).
[16] M. van der Voort, O. L. Muskens, A. V. Akimov, A. B. Pevtsov, and J. I. Dijkhuis, Phys. Rev. B **64**, 045203 (2001).
[17] S. A. Basun, P. Deren, S. P. Feofilov, A. A. Kaplyanskii, and W. Strek, J. Lumin. **45**, 115 (1990).
[18] A. A. Kaplyanskii, A. V. Akimov, S. A. Basun, S. P. Feofilov, E. S. Moskalenko, J. Kocka, and J. Stuchlik, J. Lumin. **53**, 7 (1992).
[19] K. F. Renk and J. Deisenhofer, Phys. Rev. Lett. **26**, 764 (1971).
[20] U. Buchenau, M. Prager, N. Nücker, A. J. Dianoux, N. Achmad, and W. A. Philips, Phys. Rev. B **34**, 5665 (1986).
[21] L. E. Erickson, Opt. Commun. **15**, 246 (1975).